

An Analysis of Coaxial Line Slot antenna for Hyperthermia Treatment by Spectral Domain Approach

T. Nakata, H. Yoshitake, K. Wakino, Y.-D. Lin, and T. Kitazawa
Ritsumeikan University, Japan

Abstract—An extended spectral domain approach (ESDA) is applied to evaluate the scattering parameter of laterally slotted coaxial antenna for hyperthermia treatment. The results calculated by ESDA are in good agreement with that by Finite Element Method (FEM) simulation. Computational labor of the present method is far lighter than that of FEM, and the method is suitable for the iterative computation that is required for the optimization of antenna design. The present method can afford to consider the effect of the metallization thickness in the outer conductor.

1. Introduction

In the fields of medical application, microwave is utilized for various purposes in the examining and treatment equipment [1]. The characteristics of coaxial line slot antenna for microwave hyperthermia applicators have been investigated [2]. This treatment thrusts a coaxial line applicator into the affected cancer part, heats up selectively the affected area and fixes the cancer cells. The currently used coaxial line applicator is not optimized in the point of view of impedance matching between applicator and human tissue, so that the radiation efficiency into the affected area is not good. In this paper, we analyze the radiation characteristics of applicator using efficient simulation technique and proposed the optimized design that presents high radiation efficiency.

The formulation procedure utilized in this paper is based on the extended spectral domain approach (ESDA). This procedure can afford to consider the effect of thickness of outer conductor of coaxial cable. The results calculated by ESDA are compared with that by FEM simulation and excellent agreement have been obtained between both results.

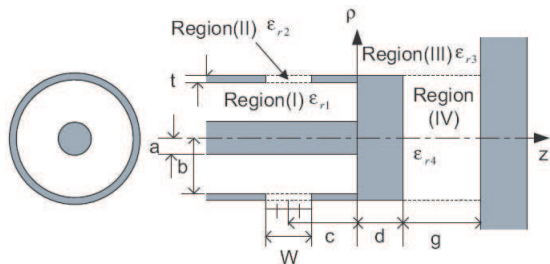


Figure 1: Schematic structure of coaxial line slot antenna.

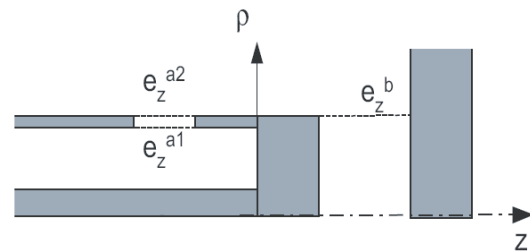


Figure 2: Aperture electric fields.

2. Theory

Figure 1 shows the schematic structure of coaxial line slot antenna whose outer conductor has finite thickness t and has a ring slot of W in width cut laterally near the termination. A perfect electric conductor (PEC) sheet is introduced for convenience of analysis in the position apart g from the tip of coaxial line. It is assumed that the relative complex permittivity of material in each region is ϵ_{r1} , ϵ_{r2} , ϵ_{r3} , ϵ_{r4} , respectively. The radiation characteristics of coaxial line slot antenna are analyzed based on the extended spectral domain approach (ESDA) [3]. In the procedure, first the aperture fields are introduced in the aperture of outer conductor designated as e_z^{a1} (at $\rho = b$), and e_z^{a2} (at $\rho = b + t$) (Fig. 2), respectively. Whole analytic space is divided into four regions, that is, region I ($a \leq \rho \leq b$, $-\infty \leq z \leq 0$), region II ($b \leq \rho \leq b + t$, $-c - w/2 \leq z \leq -c + w/2$), region III ($b + t \leq \rho \leq r$, $-\infty \leq z \leq d + g$), and region IV ($0 \leq \rho \leq b + t$, $d \leq z \leq d + g$), as shown in Fig. 1. These regions can be treated independently resorting to equivalence theorem, and the electromagnetic fields in each region are Fourier transformed with respect to the z -direction. When the dominant TEM mode

$$E_\rho = \frac{E_0}{\rho} \exp(-jk_1 z), \quad H_\phi = \sqrt{\frac{\epsilon_{r1} \epsilon_0}{\mu_0}} \frac{E_0}{\rho} \exp(-jk_1 z) \quad (a \leq \rho \leq b) \quad (1)$$

enters the coaxial line slot antenna, there exist the incident and the scattered waves in region (I) and total

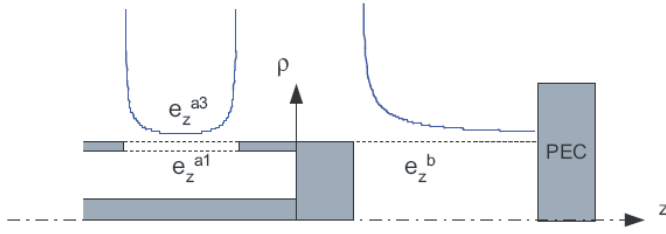
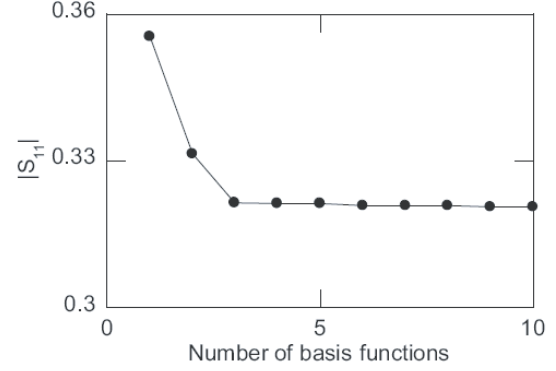


Figure 3: Edge singularities in aperture fields.

Figure 4: Convergence of the reflection coefficients with respect to number of basis functions. $a = 0.24$ mm, $b = 0.8$ mm, $c = 2.5$ mm, $d = 5.0$ mm, $w = 2.0$ mm, $t = 0.1$ mm, $\epsilon_{r1} = 2.1 - j0.0005$, $\epsilon_{r2} = \epsilon_{r3} = \epsilon_{r4} = 43 - j12.38$, $f = 2.45$ GHz.

electromagnetic fields are expressed by Fourier integrals as,

$$\begin{aligned}
 E_{\rho}^{(I)}(\rho, z) &= -j \frac{2E_0}{\rho} \sin(k_1 z) + \sqrt{\frac{2}{\pi}} \int_{-\infty}^0 \tilde{E}_{\rho}^{(I)}(\rho) \sin(\alpha_1 z) d\alpha_1, \\
 E_z^{(I)}(\rho, z) &= \sqrt{\frac{2}{\pi}} \int_{-\infty}^0 \tilde{E}_z^{(I)}(\rho) \cos(\alpha_1 z) d\alpha_1, \\
 E_{\phi}^{(I)}(\rho, z) &= \sqrt{\frac{\epsilon_{r1}\epsilon_0}{\mu_0}} \frac{2E_0}{\rho} \cos(k_1 z) + \sqrt{\frac{2}{\pi}} \int_{-\infty}^0 \tilde{H}_{\phi}^{(I)}(\rho) \cos(\alpha_1 z) d\alpha_1
 \end{aligned} \quad (2)$$

Similar expressions are available in region (III). The electromagnetic fields in regions (II) and (IV) are expressed by Fourier series instead of Fourier integrals to satisfy the boundary conditions on the side walls. Fields in regions (II) are expressed as

$$\begin{aligned}
 E_{\rho}^{(II)}(\rho, z) &= \sum_{n=1}^{\infty} \tilde{E}_{\rho}^{(II)}(\rho) \sin \alpha_2 (z + c + \frac{W}{2}), & E_z^{(II)}(\rho, z) &= \sum_{n=0}^{\infty} \tilde{E}_z^{(II)}(\rho) \cos \alpha_2 (z + c + \frac{W}{2}), \\
 H_{\phi}^{(II)}(\rho, z) &= \sum_{n=0}^{\infty} \tilde{H}_{\phi}^{(II)}(\rho) \cos \alpha_2 (z + c + \frac{W}{2}), & \alpha_2 &= \frac{n\pi}{W}.
 \end{aligned} \quad (3)$$

And similar expressions are available in region (IV).

These expressions of electromagnetic fields are substituted into Maxwells field equations. The general solutions of the transformed field equations can be expressed in terms of Bessel functions and Neumann functions in regions (I), (II) and (IV), and in terms of second kind of Hankel functions in region (III) as

$$\tilde{H}_{\phi}^{(i)}(\alpha_i; \rho) = A^{(i)} J_1(\xi_i \rho) + B^{(i)} N_1(\xi_i \rho) \quad \text{in regions(I), (II) and (IV)} \quad (4)$$

$$\tilde{H}_{\phi}^{(III)}(\alpha_3; \rho) = C^{(III)} H_1^{(2)}(\xi_3 \rho) \quad \text{in regions(III)} \quad (5)$$

where $A^{(i)}$, $B^{(i)}$ and $C^{(III)}$ are unknown constants and $\xi_i = \sqrt{\omega^2 \epsilon_{ri} \epsilon_0 \mu_0 - \alpha_i^2}$. These unknown constants can be related to the aperture fields e_z^{a1} , e_z^{a2} and e_z^b by applying the continuities of electric fields at interfaces. Then the electromagnetic fields in each region are expressed in terms of the aperture fields, for example,

$$H_{\phi}^{(I)}(\rho, z) = \sqrt{\frac{\epsilon_{r1}\epsilon_0}{\mu_0}} \frac{2E_0}{\rho} \cos(k_1 z) + \int_{z'=-c-W/2}^{-c+W/2} Y^{(I)}(\rho, z|z'=b, z') e_z^{a1}(z') dz' \quad \text{in region(I)} \quad (6)$$

where $Y^{(I)}$ is the Green's function and it can be derived easily in the transformed domain. Similar expressions are derived in other regions, which relate the fields to the involved aperture fields. The remaining boundary conditions, i. e., the continuity of the magnetic field at the interfaces between adjacent regions, are applied to obtain a set of the integral equations on the aperture fields. The aperture fields can be determined by applying

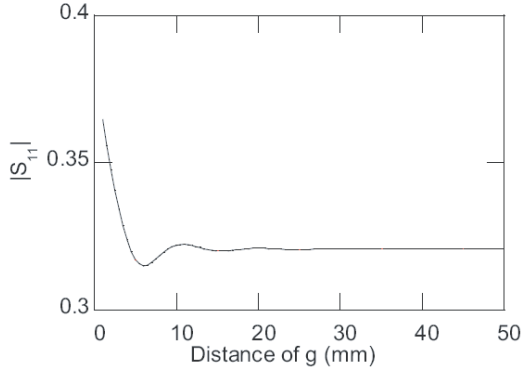


Figure 5: Convergence of reflection coefficients with respect to the distance of g . $a = 0.24$ mm, $b = 0.8$ mm, $c = 2.5$ mm, $d = 5.0$ mm, $w = 2.0$ mm, $t = 0.1$ mm, $\epsilon_{r1} = 2.1 - j0.0005$, $\epsilon_{r2} = \epsilon_{r3} = \epsilon_{r4} = 43 - j12.38$, $f = 2.45$ GHz.

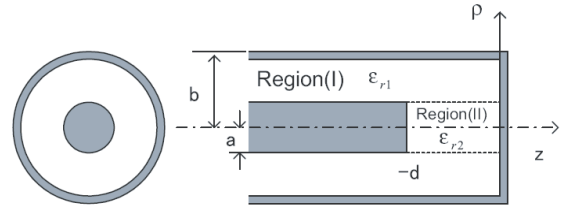


Figure 6: Gap discontinuity in coaxial line.

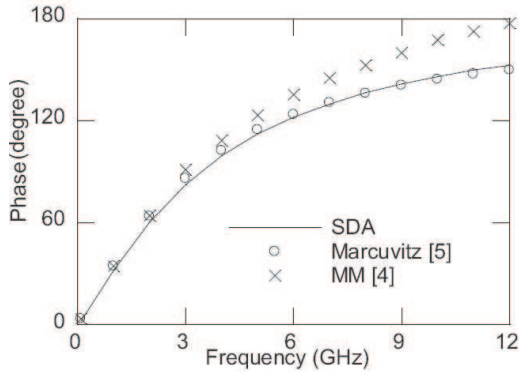


Figure 7: Phase variation of the reflection versus the frequency. $a = 3.10$ mm, $b = 7.14$ mm, $d = 0.57$ mm, $\epsilon_{r1} = \epsilon_{r2} = 2.1$.

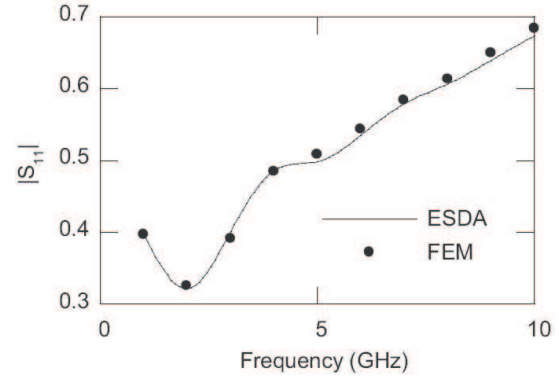


Figure 8: Frequency dependency of reflection coefficients of coaxial line slot antenna. $a = 0.24$ mm, $b = 0.8$ mm, $c = 2.5$ mm, $d = 5.0$ mm, $w = 2.0$ mm, $t = 0.1$ mm, $\epsilon_{r1} = 2.1 - j0.0005$, $\epsilon_{r2} = \epsilon_{r3} = \epsilon_{r4} = 43 - j12.38$.

the Galerkin's procedure to these coupled integral equations, and the scattering parameter (complex reflection constant) S_{11} are obtained by taking the inner product between the aperture field e_z^{a1} and the eigen function of coaxial line.

3. Numerical Procedure and Result

The numerical procedure is based on Galerkin's procedure, and the unknown electric aperture fields e_z^{a1} , e_z^{a2} and e_z^b are expanded in terms of the appropriate basis functions,

$$e_z^i(z) = \sum_{k=1}^N a_k^i f_k^i(z) \quad (7)$$

The basis functions $f_k^i(z)$ are chosen taking the edge singularities near conductor edge into consideration (Fig. 3),

$$f_k^{a1}(z) = f_k^{a2} K(z) = \frac{T_{k-1} \left\{ \frac{2}{W} (z+c) \right\}}{\sqrt{1 - \left\{ \frac{2}{W} (z+c) \right\}^2}}, \quad f_k^b(z) = \frac{T_{2(k-1)} \left\{ \frac{1}{g} (z-d-g) \right\}}{\sqrt{1 - \left\{ \frac{1}{g} (z-d-g) \right\}^2}} \quad (8)$$

where $T_k(x)$ is Chebyshev polynomials of the first kind.

Preliminary computations are carried out to investigate the convergence of the reflection coefficients with respect to the number of basis functions. This method was settled by a little number of basis functions as shown in Fig. 4, and $N = 8$ is used in the following computations. Fig. 5 examines the effect of the fictitious perfect electric conductor sheet placed at distance g ahead the tip of coaxial line slot antenna (Fig. 1). The influence of the conductor sheet decreases rapidly with g , and the sufficient spacing $g = 40$ mm is chosen in the following simulations.

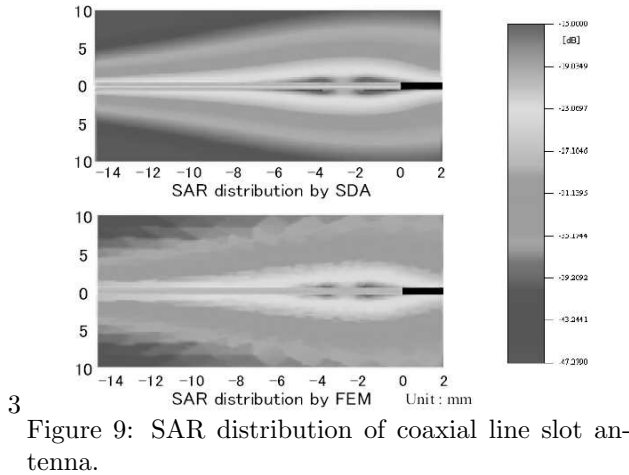


Figure 9: SAR distribution of coaxial line slot antenna.

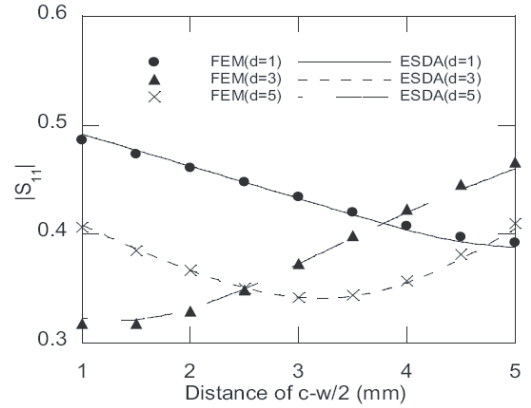


Figure 10: Variation of the reflection versus the slot position. $a = 0.24$ mm, $b = 0.8$ mm, $w = 2.0$ mm, $t = 0.1$ mm, $\epsilon_{r1} = 2.1 - j0.0005$, $\epsilon_{r2} = \epsilon_{r3} = \epsilon_{r4} = 43 - j12.38$, $f = 2.45$ GHz.

To author's knowledge there is no published theoretical result to permit direct comparison with the present method for the reflection characteristics of coaxial line slot antenna. We apply the present method to analyze the gap discontinuity in the inner conductor of shorted coaxial line (Fig. 6) to show the validity of the method. The formulation procedures are similar to those explained above and also the similar basis functions (8) are used in the numerical computation. Fig. 7 shows the phase variation of the reflection coefficient versus the frequency, comparing the results by mode-matching method [4] and Marcuvitz's analytical results [5]. Our results are in good agreement with [5] for wide frequencies.

Figure 8 shows the frequency dependency of reflection coefficients of the coaxial line slot antenna (applicator) thrust into the liver. The figure includes the values by FEM for comparison, and excellent agreement is observed between both methods over wide frequencies. Fig. 9 shows the SAR distribution calculated by both methods at $f = 2.45$ GHz.

The present method is numerically efficient and is suitable for the optimization of the coaxial line applicator, which requires the iterative computations. Fig. 10 shows the optimization of coaxial line by changing a slot position when the operation frequency is 2.45 GHz. The optimal value at this condition takes the reflective coefficient 0.32 at $c - w/2 = 1.5$ mm and $d = 5$ mm. This figure also includes the values by FEM and again good agreement is confirmed, although FEM calculations are time consuming and are presented only at discrete frequencies.

4. Conclusion

In this paper, we proposed the novel analyzing technique for the coaxial line slot antenna by ESDA, and carried out extraction of scattering parameters. This method can take the thickness effect of outer conductor into consideration. This method also secures the high accuracy by considering the singularities of fields near the conductor edge properly. The computational labor of the new method is far lighter than that of FEM, so that novel method is suitable for the time consuming iterative computation such as optimization procedure of antenna design.

REFERENCES

1. Sterzer, S., "Microwave medical devices," *IEEE Microwave Magazine*, Vol. 3, 65–70, March 2002.
2. Saito, K., Y. Hayashi, H. Yoshimura, and K. Ito, "Heating characteristics of array applicator composed of two coaxial-slot antennas for microwave coagulation therapy," *IEEE Trans. Microwave Theory Tech.*, Vol. 48, 1800–1806, November 2000.
3. Kitazawa, T., "Nonreciprocity of phase constants, characteristic impedances and conductor losses in planar transmission lines with layered anisotropic media," *IEEE Trans. Microwave Theory Tech.*, Vol. 43, 445–451, February 1995.
4. Eom, H. J., Y. C. Noh, and J. K. Park, "Scattering analysis of a coaxial line terminated by a gap," *IEEE Microwave Guided Wave Lett.*, Vol. 8, 218–219, June 1998.
5. Marcuvitz, N., *Waveguide Handbook*, New York: McGraw-Hill, 178, 1951.